



FINITE ELEMENT INVESTIGATION OF INITIAL CLEARANCE EFFECT ON TUBE-TO-TUBESHEET JOINT STRENGTH

N. Merah*¹, A. Al-Zayer², A. Shuaib¹, and A. Arif³

1: Associate Professor, Mechanical Engineering, KFUPM

2: PD&CD/CADSD, Saudi-ARAMCO

3: Assistant Professor, Mechanical Engineering, KFUPM

E-mail: nesar@kfupm.edu.sa

ABSTRACT

The tube-to-tubesheet joint strength is measured in terms of residual contact pressure between the tube's outer surface and tubesheet hole surfaces. The joint integrity is affected by several design parameters, including the type of material and the initial radial clearance. To avoid weakening of joints due to excessive initial radial clearances Tubular Exchanger Manufacturer Association (TEMA) has set standards in which maximum over-tolerances are spelled out.

The present work complements the experimental program on the effect of over-tolerance on heat exchangers tube-to-tubesheet joint strength. The finite element analysis first addressed the ligament effect on the residual stress in order to select a satisfactory sleeve diameter. Second, the initial clearance effect on contact pressure and percent tube wall reduction is performed. Results show that for low strain hardening materials the initial clearance effect is negligible. However, higher levels of strain hardening have a significant effect on residual stress and percent wall reduction. For low clearances, the finite element estimated residual contact pressure compared well with the analytical result and that inferred from the experimentally measured pull-out force. The variation of the percent wall reduction with initial clearance is found to be similar to that of the measured one.

Keywords: joint-strength, contact pressure, tube-sheet, radial clearance, over-tolerance, FEM.

المخلص

(TEMA)

1. INTRODUCTION

The tube-to-tubesheet joint is a very critical element of the shell-tube heat exchangers. It separates the two fluids and thus its strength level has a direct effect on the safety of the process plant. This joint is made by either expansion, welding or a combination. However, tube expansion is mostly used in industry, since Tubular Exchanger Manufacturer Association (TEMA) standard [TEMA, 1988] calls for tube expansion joints. Tube expansion is done by rolling, uniform (hydraulic) pressure, bladder, rubber, explosive or hybrid expansion. Among all these kinds of expansion, rolling is the most common kind in the industry. Since it is the easiest and cheapest. In the expansion process, the tube deforms plastically and the tubesheet often deforms elastically after which tubesheet reverse deformation is more than that of the tube and causes permanent contact.

To get a strong tube-tubesheet joint, certain limitations specified by TEMA have to be applied. Among these limitations is the maximum allowable initial radial clearance between the tube and tubesheet, which is specified in terms of over tolerance. Table RCB-7.41 in the TEMA standards [TEMA, 1988] lists this limitation for each tube size. Tube expansion into tubesheet holes having more than the allowable radial clearance (over tolerance) may stretch the tubes beyond their strain limit or may cause tube wall reduction to be more than a pre-specified acceptable limit. According to Yokell [Yokell, 1991], roller-expanded joints are generally rejected when tube wall reductions approach 12%, since resultant joint would be weak and may fail under working pressure.

The tube-to-tubesheet joint strength is measured by the residual contact pressure between the tube's outer surface and tubesheet's hole surface or by the pull or push out force needed to draw the tube apart from the tubesheet. Both measures are directly related. Several studies to estimate this joint strength and how it is affected by changing different parameters involved are already published [Sang et al, 1996; Scott et al, 1984; Updike et al, 1992, Kasraie et al, 1983; and Jawad et al, 1987]. The effect of grooves was studied by Sang and co-workers [Sang et al, 1996] and by Scott et al [Scott et al, 1984]. These authors concluded that the presence of grooves give the joint additional locking mechanism. Jawad and co-workers [Jawad et al, 1987] have investigated the hole surface condition effect on the strength of steel-steel joints and found that it is improved by roughness. However, the effect of initial radial clearance on the joint strength was not thoroughly addressed. Fisher and Brown [Fisher and

Brown, 1954] experimentally investigated the effect of oversized tube-hole on rolled joint integrity. They found that the negative effect of initial clearances up to 0.008 in. (0.203 mm) could be overcome by proper rolling. Allam and co-workers [Allam et al, 1998] conducted a Finite Element Analysis (FEM) of the effects of clearance and material strain hardening on the interfacial pressure. They concluded that the clearance effect is significant for high level of strain hardening materials. More recently, Shuaib et al [Shuaib et al, 2001, a] performed an experimental investigation of steel-steel joint strength and found that clearances up to 0.015 in. did not have a major effect on the pull-out force.

The objective of this study is to investigate the effect of initial radial clearance and material strain hardening on the strength of the expanded tube-to-tubesheet joint by using finite element method (FEM). The study involves numerical estimation of the residual contact pressure and percent tube wall reduction through the use of a general finite element code [ANSYS, 1999]. It uses the same model geometry and base line data presented in the experimental work conducted by Shuaib and co-workers [Shuaib et al, 2001, b]. The temperature effect on the joint strength is not considered in the present study. It is known that this effect is negligible in the operating conditions of the investigated heat exchanger.

2. FINITE ELEMENT MODEL

The test block simulating the tubesheet hole design configuration of the stabilizer feed/bottom exchanger used in the experimental work [Shuaib et al, 2001, b] is modeled and analyzed hereafter. Figure 1, illustrates the geometry and dimensions of the block. The test assembly was designed to ensure that the effect of ligament on the test joint (the center hole) is accounted for. The material of the sheet was carbon steel ASTM A516 G70 ($\sigma_{ys} \approx 37.5$ ksi, (261 MPa)). A standard $\frac{3}{4}$ nominal diameter tubes with an average outer radius (r_o) of 0.3745 in. (9.5123 mm) and inner radius (r_i) of 0.2863 in. (7.272 mm) were expanded in each hole. All the tubes were cut from the seamless cold-drawn low carbon steel type, ASTM 179 ($\sigma_{yt} \approx 36$ ksi, (248 MPa)).

The equivalent sleeve concept is implemented in this study where finite element code (ANSYS) is used to predict the effect of initial radial clearance on the residual contact pressure. A preliminary analysis was performed to validate the use of a simplified single hole model. It was found that the equation proposed by Chaaban et al [Chaaban et al, 1992] results in a good estimate of the contact pressure. Using the block dimensions together with the material specifications (sheet and tube moduli: $E_s = E_t = 30 \times 10^3$ ksi (207 GPa) and yield stresses: $\sigma_{ys} = \sigma_{yt} = 36$ ksi, (248 MPa)) yielded an equivalent sleeve radius (R_o) of 1.4165 in. (36 mm). The values of the yield stresses of sheet and tube are taken to be equal to 36 ksi, (248 MPa), to simplify the model. The resulting equivalent single hole axisymmetric model dimensions are shown in Figure 2. The initial radial clearance is illustrated on the figure.

Besides the axisymmetric model, a single hole planar model is developed using the same radial dimensions. Due to the all around symmetry and to reduce the computational time, only a quarter circle was modeled and analyzed. This model is used to perform both plane stress and plane strain analyses.

A higher order quadrilateral two-dimensional eight-nodes isoparametric element (PLANE82) was selected. This 8-nodes element is well suited to model curved boundaries and can be used as a planar element or as an axisymmetric element. It has plasticity, stress stiffening, large deflection, and large strain capabilities. CONTA172 and TARGE169 elements are used to represent flexible-to-flexible surface-to-surface contact between the deformable surfaces on the tube and tubesheet. Using these elements, clearances, c , ranging from 0.000 to 0.004 in. (0.000 to 0.1016 mm) were modeled and studied.

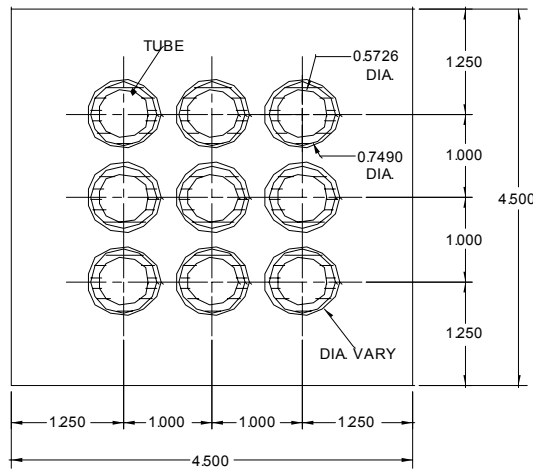


Figure 1: Model Geometry and Dimensions in inches.

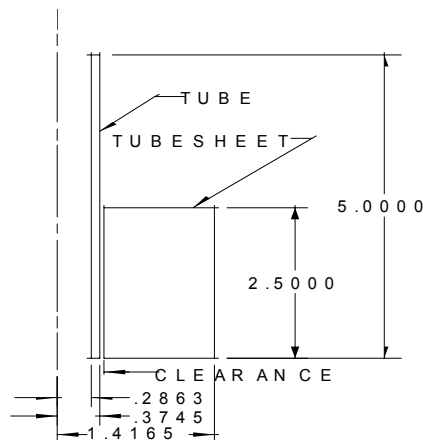


Figure 2: Axisymmetric Model Showing Clearance (Dimensions in inches)

The finite element meshes and models for both axisymmetric and planar model are shown respectively in figures 3 and 4 along with the boundary conditions and the applied pressure.

A bilinear representation of the true stress-strain curve of the tube material was made. The plastic region of tube material behavior was approximated by a line having a slope (tangent modulus) of 127,000 psi (0.876 GPa). However, to investigate the material's strain hardening effect on the residual pressure the tube's tangent modulus (E_{tt}) was varied to take these values, 0.1×10^6 , 0.5×10^6 and 1.0×10^6 psi (0.69, 3.45 and 6.9 GPa). These values were chosen to cover most of the steel materials. The other material properties specified in the finite element code are a Poisson's ratio of 0.3 and frictional coefficient of 0.74. It should be mentioned that, the effect of coefficient of friction on the residual contact pressure was investigated and found to be negligible [Al-Zayer, 2001].

Internal pressure was applied in several load steps. As the tube starts to come into contact with the hole surface more load steps are used to overcome the associated nonlinearities. In the axisymmetric model, the pressure is applied from the tubesheet's primary side ($y = 0$ in.) to the secondary side ($y = 2.5$ in. (63.5mm)). A maximum expanding pressure of 36000 psi (248 MPa) was used in all the analyses.

3. RESULTS AND DISCUSSION

3.1 Residual Contact Pressure

A typical residual contact pressure distribution at the end of expansion process along longitudinal direction for the case of 0.002 in (0.051 mm) initial radial clearance and tube's tangent modulus (E_{tt}) of 500,000 psi (0.345 GPa) is shown in Fig. 5. This case was selected for demonstration because it falls in mid-range of the initial radial clearances and tube's tangent moduli covered in this study. The contact pressure shown in Fig. 5 is constant, with a value of about 3300 psi (22.8 MPa), through out the tube length extending from $y = 0$ in. to $y = 1.73$ in (44 mm). This length corresponds to about 70% of the expanded tube portion. The contact pressure then starts to decrease very slightly before it shoots up to its maximum of 6304 psi at the approximate location of $y = 2.28$ in. (58 mm) Then it falls down to zero just below the secondary side ($y = 2.5$ in. (63.5 mm)) where the expansion pressure ended.

The above described residual contact pressure distribution is common for all the non-zero initial radial clearance cases covered in the study. However, this phenomenon was not observed in the zero clearance case. In this case, the contact pressure is constant through out the section extended from the tubesheet's primary side to a point just below the secondary side where it starts to drop down gradually to a small value (Fig. 6). It is important to note that the value of the residual contact pressure to be illustrated later for all the cases covered in this study is the uniform pressure that takes place in the major part of the expanded tube length. This is the pressure extending from the primary side ($y = 0$ in.) to the point below the secondary side at which the pressure starts to drop down.

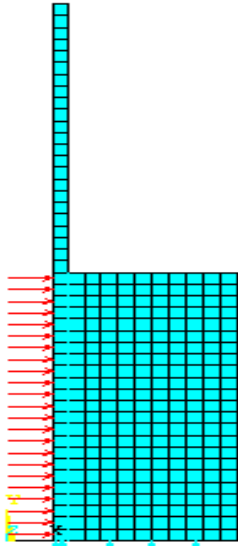


Figure 3: Meshed Axisymmetric Model

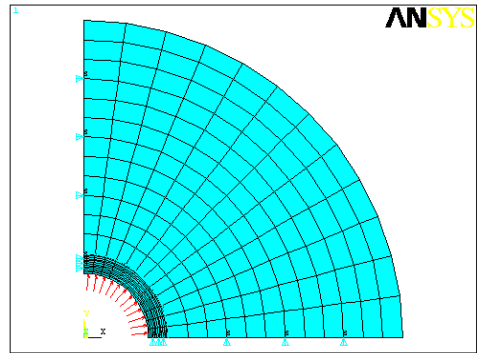


Figure 4: Meshed Planar Model

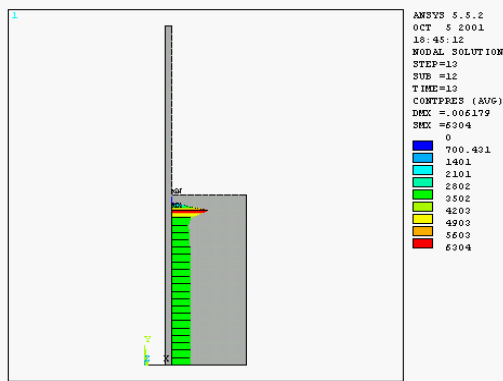


Figure 5: Longitudinal Contact Pressure Distribution

Distribution For The Case $c = 0.002$ in.

$E_{tt} = 500000$ psi ($c=0.0508$ mm,
 $E_{tt} = 0.345$ GPa).

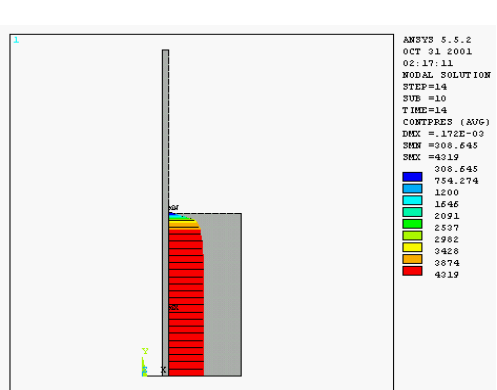


Figure 6: Longitudinal Contact Pressure Distribution

For The Case $c = 0.0$ in.,

$E_{tt} = 500000$ psi ($c=0$ mm,
 $E_{tt} = 0.345$ GPa).

The peak value of the residual contact pressure occurring below the secondary side in the cases where the initial radial clearance is not zero can be explained by noting that a smooth transition, like an S shape, will occur between the expanded and unexpanded portions of the tube. As a result, the tube surface in transition zone will concave. The applied pressure will

always act perpendicular to the line surface on which it is applied. So, the pressure will follow the curved tube surface and make the tube bow more and more until it comes in contact with the tubesheet. This behavior is investigated in detail in the work by Al-Zayer [Al-Zayer, 2001]. After contact, the tubesheet wall will act to flatten the concaved surface and thus higher pressure will be exerted on the tubesheet hole surface in that location. When the pressure is released, residual contact pressure will be maximum in this location.

All the tube retraction is expected to occur on the free end, because the tube and tubesheet were restrained in the axial direction on the primary side. This retraction is responsible for the zero contact pressure occurring at the secondary side. For the case of zero initial radial clearance, there will be no concaved surface that would exert more pressure on the tubesheet. So, a peak contact pressure value was not observed at the secondary side.

On the other hand, the circumferential contact pressure distribution obtained from the planar model, is uniform all around the tube-tubesheet joint with a value of 3450 psi. This is the case for both plane stress and plane strain analyses where $c = 0.002$ in and $E_{tt} = 500,000$ psi.

The residual contact pressures for the three models and the three values of tube's tangent modulus are plotted versus initial radial clearance in Figure 7. As it can be seen from the figure, a linear relationship exists between the residual contact pressure and the initial radial clearance for a given tangent modulus (E_{tt}) value for the three models. The decrease in the residual contact pressure is higher for the larger tube's tangent modulus. As E_{tt} approaches zero, which is the case of elastic-perfectly-plastic material, the contact pressure will retain a constant value regardless of the radial clearance. In other words, the residual contact pressure will be independent of the initial radial clearance.

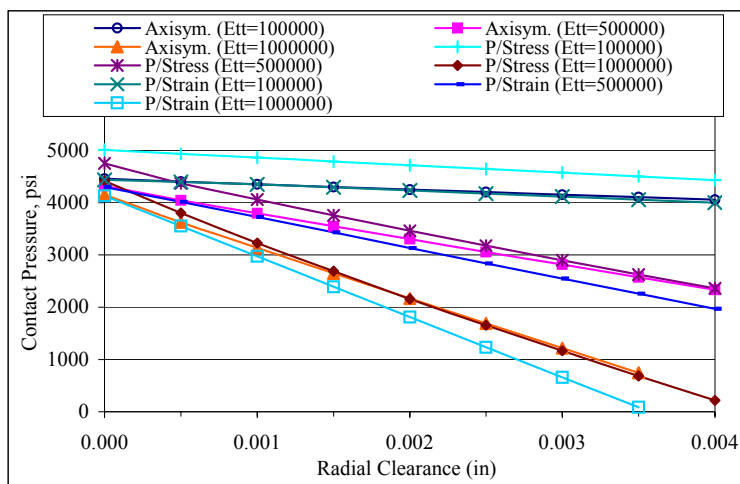


Figure 7: Residual Contact Pressure Variation with Clearance

Following the parametric study conducted by Allam and co-workers [Allam et al, 1998], the variables of interest will be non-dimensionlized to generalize the analysis. The pressure will be normalized by the yield strength, the clearance by the tube’s outer radius and the tangent modulus by the modulus of elasticity. The residual contact pressure results for the range of initial radial clearances and tangent modulii covered in this study obtained from the axisymmetric model will be utilized to generate the nondimensional parametric analysis.

As can be seen from Fig. 7, both E_{tt} and c have a significant negative effect on the residual contact pressure. To account for their effect, a reduction factor is introduced into the analytical solution because in the analytical calculation of the residual interfacial pressure, P_{con} , it is assumed that the material is elastic-perfectly-plastic ($E_{tt} = 0$) and the initial radial clearance is neglected ($c = 0$). Using the formula proposed by Yokell [Yokell, 1991] for the case where tube and tubesheet materials have equal yield stresses P_{con} is calculated as follows:

$$P_{con} = P_e \left[1 - \left(\frac{r_i}{r_o} \right)^2 \right] - \left(\frac{2}{\sqrt{3}} \right) \sigma_y \left[\ln \left(\frac{r_o}{r_i} \right) \right] \tag{1}$$

Where r_i is the inner radius of the tube, σ_y is the yield stress of the tube determined from the tensile tests to be 36 Ksi (248 MPa), P_e is the expanding pressure estimated using the following equation given by the same author [Yokell, 1991]:

$$P_e = \sigma_y (1.945 - 1.384 r_i/r_o) \tag{2}$$

The analytically calculated residual contact pressure for the dimensions and material properties used in this study was found to be 4434 psi (30.6 MPa). The average value of the residual stress calculated using FEM for zero clearance and tangent modulus of 100,000 psi (690 MPa) is 4459 psi (30.8 MPa).

The reduction factor (z) for each case covered in this study can then be found by dividing the residual contact pressure obtained from the finite element analysis by 4434 psi (30.6 MPa). To express the combined effects of both parameters, the normalized clearance is multiplied by the normalized tangent modulus to have a non-dimensional parameter $\left(\frac{c}{r_o} \times \frac{E_{tt}}{E_t} \right)$. The reduction factor due to grouping c and E_{tt} for each case is plotted with respect to this non-dimensional parameter in Fig. 8.

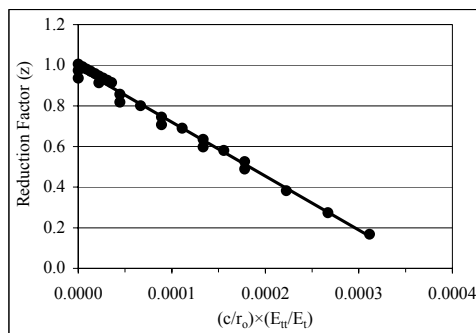


Figure 8: Reduction Factor of Combined Clearance and Tangent Modulus Effect

The figure shows that the variation of z with $\left(\frac{c}{r_o} \times \frac{E_{tt}}{E_t}\right)$ can be expressed by the following linear relationship:

$$z_{(c \& E_{tt})} = 1.0 - 2770 \frac{c}{r_o} \frac{E_{tt}}{E_t} \quad (3)$$

As explained earlier, the initial radial clearance value does not affect the residual contact pressure if an elastic-perfectly-plastic material is assumed. This means that the reduction factor will be equal to 1.0 for this case. Equation (3) will successfully give this result when E_{tt} is set to zero. However, this equation will also give a unity reduction factor when the initial radial clearance is zero, regardless of the tangent modulus value. This is not true. As the tangent modulus level increases, the tube material becomes harder and exerts more resistance to the applied pressure. Since the applied pressure is fixed for all the cases in the study, resultant pressure on the tubesheet hole surface will be less because more pressure has been taken by the tube. As a result, the residual contact pressure will decrease as the level of tube tangent modulus increases.

To make the necessary correction in Eq. (3), the effect of the tangent modulus on the residual contact pressure was studied for the case of zero initial radial clearance. An axisymmetric model having zero clearance was generated and the tangent modulus was changed in the range of 0 to 10×10^6 psi (0 to 69 GPa). A linear relationship was found between the reduction factor and the non-dimensional parameter $\left(\frac{E_{tt}}{E_t}\right)$ and again the line intersects the ordinate at a value of 1.0. This line has a negative slope of 1.7, which means that the reduction factor on the residual contact pressure of a tube-tubesheet joint having zero initial radial clearance is given by:

$$z_{(E_n)} = 1.0 - 1.7 \frac{E_{tt}}{E_t} \tag{4}$$

To arrive at a single formula for estimating the reduction factor applicable for any combination of the initial radial clearance and tangent modulus, the reduction factor due to E_{tt} alone is added to the reduction factor due to grouping c and E_{tt} for each case. The resulting values are plotted in Figure 9.

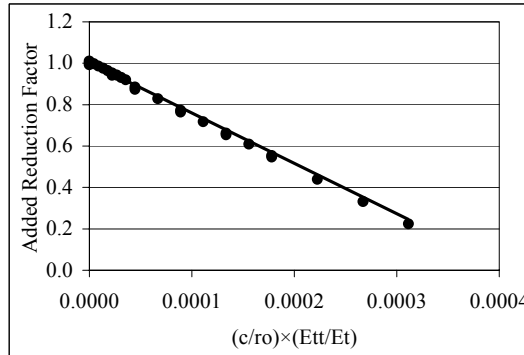


Figure 9: Added Reduction Factor

The combined effects can be described by the following general linear relationship:

$$z = 1.0 - 2500 \frac{c}{r_o} \frac{E_{tt}}{E_t} - 1.7 \frac{E_{tt}}{E_t} \tag{5}$$

It should be noted here that the correction factor proposed by Allam and co-workers [Allam et al., 1998] did not include the effect of material strain hardening on residual contact pressure for zero clearance.

The results concerning the effect of initial radial clearance on the residual contact pressure obtained by finite element analysis were compared to those inferred from the pull out force measured experimentally. It was found that the general trend of constant pull out force obtained for all the range of clearances is justifiable given that the tangent modulus of the material is only 127,000 psi. (876 MPa) As can be seen in Fig. 7 and from Eq. 5 the clearance effect for this range of E_{tt} is negligible. The average value of the contact pressure inferred from the experimental pull-out force was within 15% of that determined from FEM.

3.2 Tube wall reduction

In the industry, tube wall reduction is a very important measure and it may be a basis for rejecting equipment if the tube wall has reduced more than a pre-specified value. Normally, tube wall reduction caused by roller expansion is 3 to 12%, whereas it is 1 to 3% when expansion is performed by applying uniform pressure [Yokell, 1992].

Since it is not practical to measure the wall thickness after expansion, tube wall reduction is calculated by the following formula:

$$WR = \frac{(r_{i,f} - r_i) - (R_i - r_o)}{(r_o - r_i)} \times 100 \quad (6)$$

Where, WR is percent tube wall reduction, r_i is the tube inner radius before expansion, $r_{i,f}$ is the tube inner radius after expansion, r_o is tube outer radius before expansion and R_i is tubesheet hole radius before expansion.

The wall reduction calculated by equation (6) is named “apparent wall reduction” because it does not account for the radial ligament deformation. Only the inner tube radius after expansion needs to be measured. However, since the tube radius can not be read directly from the finite element code, it would be more practical to express equation 6 in terms of radial deformation. By doing so, tube wall reduction formula is re-written in the following form:

$$WR = \frac{U_{ri} - c}{t} \times 100 \quad (7)$$

Where U_{ri} is radial deformation of the tube’s inner surface and t is the initial tube wall thickness.

The radial deformation of the tube’s inner surface is calculated using the three models and the percentage tube wall reduction is calculated from equation (7). Figure 10 is a plot of the percentage tube wall reduction versus initial radial clearance, for the three levels of tube’s tangent modulus.

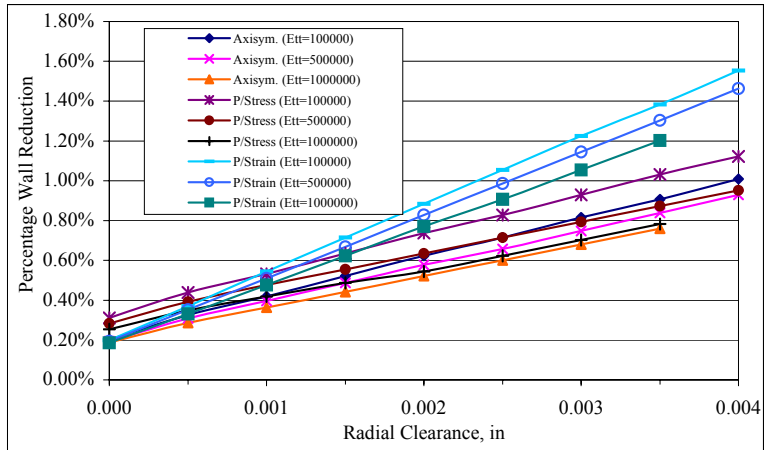


Figure 10: Percentage Tube Wall Reduction

The tube wall reduction decreases as the tangent modulus increases and, increases as the initial radial clearance increases. In the range of initial radial clearances (c) and tube's tangent modulus (E_{tt}) covered in this study, the maximum tube wall reduction, for the case having the highest clearance and lowest tangent modulus, was 1.55% resulting from the plane strain analysis. An axisymmetric analysis of the same case resulted in a wall reduction of 1.01% only. This value is below the normal maximum acceptable percentage wall reduction, which is 3% for uniformly expanded tube.

It should be noted that similar behavior of the percentage wall reduction with the over-tolerance was obtained in the experimental work performed by Shuaib and co-workers [Shuaib et al, 2001, b].

4. CONCLUSIONS

The finite element code (ANSYS) was utilized to analyze the tube-tubesheet joint strength of a stabilizer feed/bottom exchanger. A representative block was selected and a multi-hole model having the same configuration as the test block used in the experimental program was analyzed to validate the use of the simplified single-hole models. Axisymmetric, plain strain and plain stress models were used to determine the residual contact pressure distribution and tube deformation. The combination of the effects of the initial clearance and material strain hardening properties on the tube wall reduction was also studied.

The findings may be summarized as follows:

1. There is practically no initial clearance effect on contact pressure for low strain hardening material. The residual contact pressure between the uniformly expanded tube-to-tubesheet joint decreases linearly with the initial radial clearance for strain-hardening materials. As the tube's tangent modulus increases, the contact pressure becomes more sensitive to the clearance. The FE results are used to partially explain the experimental findings concerning the insensitivity of the pull-out force to the initial clearance.
2. The available closed-form solutions of the residual contact pressure that ignore the initial radial clearance and tube strain hardening can be corrected by introducing a reduction factor accounting for these two parameters. A correlation for calculating the reduction factor was developed from the results of the finite element analyses.
3. Similar to the experimental results, tube wall reduction, calculated from the radial deformation, was found to increase with increasing clearance and material strain hardening.

ACKNOWLEDGMENTS

The authors acknowledge the support of King Fahd University of Petroleum and Minerals, Saudi Arabia.

REFERENCES

1. Allam, M.; Bazergui, A. and Chaaban, A., 1998, 'The Effect of Tube Strain Hardening Level on the Residual Contact Pressure and Residual Stresses of Hydraulically Expanded Tube-to-Tubesheet Joint', *Proceedings, of the ASME Pressure Vessel and Piping Conference*, 375, pp. 447-455.
2. Al-Zayer, A., 2001, "Analytical and Finite Element Investigation of Initial Clearance Effect on Tube-Tubesheet Joint Strength", M. S. Thesis, King Fahd University of Petroleum & Petroleum, Dhahran, Saudi Arabia.
3. ANSYS, Version 5.5, Swanson Analysis System, Inc.
4. Chaaban, A.; Ma, H. and Bazergui, A., 1992, 'Tube-Tubesheet Joint: A Proposed Equation for the Equivalent Sleeve Diameter Used in the Single-Tube Model', *ASME Journal of Pressure Vessel Technology*, 114, pp. 19-22.
5. Fisher, F. F. and Brown, G. J., 1954, "Tube Expanding and Related Subjects", *Transaction of the ASME*, pp. 563-575.
6. Jawad, M. H.; Clarkin, E. J. and Schuessler, R. E., 1987, "Evaluation of Tube-to-Tubesheet Junctions", *ASME Journal of Pressure Vessel Technology*, Vol. 109, pp. 19-26.

7. Kasraie, B; Porowski, J. S.; O'Donnell, W. J. and Selz, A., 1983, "Elastic-Plastic Analysis of Tube Expansion in Tubesheet", *ASME Paper no. 83, PVP-71, Pressure Vessel and Piping Conference, Portland*.
8. Sang, Z. F.; Zhu, Y. Z. and Widera, G. E. O., 1996, "Reliability Factors and Tightness of Tube-to-Tubesheet Joints", *ASME Journal of Pressure Vessel Technology*, Vol. 118, pp. 137-141.
9. Scott, D. A.; Wolgemuth, G. A. and Aikin, J. A., 1984, 'Hydraulically Expanded Tube-to-Tubesheet Joints', *Transactions of the ASME*, Vol. 106, pp. 104-109.
10. Standards of the Tubular Exchanger Manufacturer Association 'TEMA', Seventh Edition, 1988.
11. Shuaib, A. N., Merah, N., and Allam, I. 2001, 'Investigation of Heat Exchanger Tube Sheet Hole Enlargement', ME2203 Final Report, King Fahd University of Petroleum & Petroleum, Dhahran, Saudi Arabia.
12. Shuaib, A. N., Merah, N., and Allam, I., Kheraisha, M. and Al-Anizi, S., 2001, 'Experimental Investigation Of Heat Exchanger Tube Sheet Hole Enlargement', *Proc. ASME Pressure Vessel and Piping Conference*, July 22-26,; Atlanta, Georgia.
13. Updike, D. P.; Kalnins, A. and Caldwell, S. M., 1992, "Residual Stresses in Transition Zones of Heat Exchanger Tubes", *ASME Journal of Pressure Vessel Technology*, Vol. 114, pp. 149-156.
14. Yokell, S., 1991, 'Expanded, and Welded-and-Expanded Tube-to-Tubesheet Joints', *TEMA Technical Committee Meeting*, San Francisco.
15. Yokell, S., 1992, "Expanded, and Welded-and-Expanded Tube-to-Tubesheet Joints", *ASME Journal of Pressure Vessel Technology*, 114, pp. 157-165.